

Investigation of Effects of Digital Image Processing on Improvement of Images Acquired with a Fiber-Optic Plate Microscope System

Masahiko HIRANO*, Yutaka YAMASHITA** and Atsuo MIYAKAWA***

*The Third Department of Internal Medicine, Hamamatsu University School of Medicine,
Handacho, Hamamatsu 431-31, Japan

**Hamamatsu Photonics K. K., 5000, Hirakuchi, Hamakita 434, Japan

***Photon Medical Research Center, Hamamatsu University School of Medicine,
Handacho, Hamamatsu 431-31, Japan

Effects of digital image processing on improvement of images acquired with a fiber-optic microscope system were estimated. A raw image of cultured cells stained with a fluorescent dye was noisy and had insufficient contrast for observation of a detailed image. To improve the image quality, two series of techniques were performed. For observations of static specimens, integration of consecutive frames was effective in reducing the random noise. Histogram transformation operations improved the contrast of the integrated images, providing a clearer detailed image. For observations of moving specimens, spatial filtering for smoothing the image acquired by freezing one frame was effective in reducing random noise. The contrast of the image was also enhanced with the same histogram transformation operations. Spatial filtering for the purpose of sharpening images enhanced the partition patterns of optical fibers constituting the fiber-optic plate. They were successfully removed by two-dimensional fast Fourier transform.

Keywords Fiber-optic plate microscope, video microscopy, digital image processing

Recently a new type of video-microscope system which employs a needle-shaped fiber-optic plate has been developed.¹ The fiber-optic plate consists of thousands of fine optical fibers. In this fiber-optic plate microscope system, an image at an area adjacent to the end of the fiber-optic plate is transmitted to an objective lens and then detected by a video camera. A recent study demonstrated that this system had sufficient sensitivity and resolution to make visible a single cell stained with a fluorescent dye.¹ The change in intracellular free calcium concentration, which is one of the parameters used to estimate the physiological activity of cells, could also be measured with this system. These results suggest the possibility that insertion of a fiber-optic plate will enable the internal tissues of a living animal to be visible at the single cell level and that their physiological activity will be measurable in real time.

Imaging of weak light such as fluorescence, however, tends to have insufficient signal-to-noise ratio and contrast. This inferior image quality prevents detailed observation of a specimen. In such cases, image processing for improving the image quality is required. Many digital image processing techniques have been designed up to now for various purposes, such as noise reduction, contrast enhancement and feature extraction.^{2,3} In this research, some of these image processing techniques were tried in order to improve fluorescence

images obtained with the fiber-optic plate microscope system; their effects were also investigated.

Materials and Methods

Fiber-optic plate microscope system

The structure of the fiber-optic plate microscope system used here was presented by Hirano *et al.*¹ The needle-shaped fiber-optic plate, which consists of approximately 100000 optical fibers 3 μm in diameter, was located in front of an objective lens facing the specimen. Through the fiber-optic plate, fluorescence emitted from the specimen was transmitted to a 40 \times objective lens (DPlanApo UV40, numerical aperture, 0.85, Olympus Optical Co., Ltd., Tokyo, Japan). The fluorescence images were detected by an intensified charge-coupled device (ICCD) camera (C2400-87, Hamamatsu Photonics K.K., Hamamatsu, Japan). They were then digitized by an image processor (ARGUS-50, Hamamatsu Photonics) and stored in frame memories (512 \times 483 pixels, 16 bits). Some of the functions provided by the image processor, such as spatial filtering and histogram transformation, were used in this study. The raw and the processed images were displayed on a video monitor.

Materials

Acridine Orange, Dulbecco's modified Eagle's medium (DMEM) and dibutyryl adenosine 3',5'-cyclic monophosphate (dibutyryl cAMP) were purchased from Sigma Chemical Co. (MO, USA). Newborn fetal calf serum was purchased from Mitsubishi Kasei Co. (Tokyo, Japan). *N*-2-Hydroxyethylpiperazine-*N'*-2-ethanesulfonic acid (HEPES) was purchased from Dojindo Laboratories (Kumamoto, Japan). Fluorescent beads (Fluoresbrite) were purchased from Polysciences Inc. (PA, USA). Other chemicals were purchased from Wako Pure Chemical Ind., Ltd. (Osaka, Japan).

Acquisition of fluorescence images

Cultured cells stained with a fluorescent dye and fluorescent beads were used as specimens for imaging with the fiber-optic plate microscope system. NG108-15 cells⁴, which are a hybrid cell line between the neuroblastoma and the glioma, were cultured at 37°C in DMEM containing 5% newborn fetal calf serum under a humidified atmosphere with 5% CO₂. To induce neuron-like differentiation, the cells were maintained in the medium containing 1 mM dibutyryl cAMP for 4–6 d. They were then incubated in 5 µg/ml of Acridine Orange in a medium consisting of 20 mM HEPES (pH 7.4), 115 mM NaCl, 5.4 mM KCl, 0.8 mM MgCl₂, 1.8 mM CaCl₂ and 13.8 mM D-glucose for 10 min at room temperature. After the cells were washed, they were illuminated at 490 nm (bandwidth, 7.3 nm) and fluorescence longer than 520 nm was detected. One frame of their image was stored. Immediately after the storage, the image of the same cells was obtained by integration of 64 consecutive frames. Dark noises of the ICCD camera were then subtracted from both of the images.

Fluorescent beads whose excitation maximum was 458 nm were observed. Their mean diameter was 9.4 µm. They were illuminated at 450 nm (bandwidth, 6.5 nm) and fluorescence longer than 520 nm was detected. The fluorescence images were acquired by integration of 64 consecutive frames, followed by dark noise subtraction.

Digital image processing

Some digital image processing techniques were performed in order to estimate their effects on image improvement. These techniques were successfully performed as shown in Fig. 1.

Two types of operation for histogram transformation were performed to enhance contrast of the images.³ In these operations, the slope of the original, linear gray scale of the image was modified. The first operation was gamma correction, whereby gray values of an original image (IN) were replaced by Eq. (1) at 8 bits or 256 gray levels (Fig. 2a):

$$\text{OUT} = 255 \times (\text{IN}/255)^c. \quad (1)$$

By means of this operation, depending on the value of

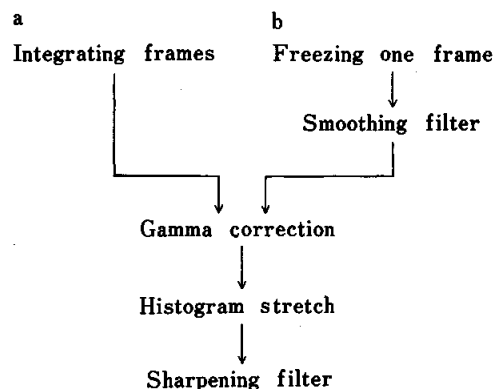


Fig. 1 Procedures for digital image processing. a. The image processing sequence for observations of static specimens. A few seconds may be required to integrate frames for noise reduction. b. The image processing sequence for observation of a moving specimen. In observations requiring high temporal resolution. The smoothing filter was used on the image acquired by freezing one frame in order to reduce random noises.

parameter (G), contrast of either a part of the low gray level in the image or that of the high gray level was enhanced.

The second type of histogram transformation was histogram stretch. In this operation, gray values in an original image (IN) were replaced by Eq. (2):

$$\text{OUT} = 255 \times (\text{IN} - I_{\min}) / (I_{\max} - I_{\min}). \quad (2)$$

In this operation, gray levels of the restricted region (from I_{\min} to I_{\max}) which were appropriately selected in the original image were linearly expanded to the full gray levels, that is, from black (intensity, 0) to white (intensity, 255) at 8 bits. Gray values of less than I_{\min} and those of more than I_{\max} were replaced by 0 and 255 respectively (Fig. 2b).

Spatial filtering techniques were used to enhance edges of specimens and also to smooth the images. To perform these techniques, a gray value of a target pixel was reassigned by operations using a convolution mask and gray values of the neighboring 3×3 or 5×5 pixels. The operations were implemented as described by Inoué.³ The 3×3 convolution mask shown in Fig. 3a was used for enhancing edges of specimens (sharpening filter). This filter has the effect of adding an image processed by a Laplacian filter, which detects edges of specimens, to the original image.

Two types of spatial filtering were performed for reducing noises occurring in the image (smoothing filter). With the 5×5 convolution mask shown in Fig. 3b, a gray value of a target pixel was replaced by the average value of the 5×5 neighboring pixels (averaging filter). The alternative smoothing filter was a median filter. This filter rearranged gray values of the neighboring 5×5 pixels in the order of their intensity and output the median value as a value of the target pixel.

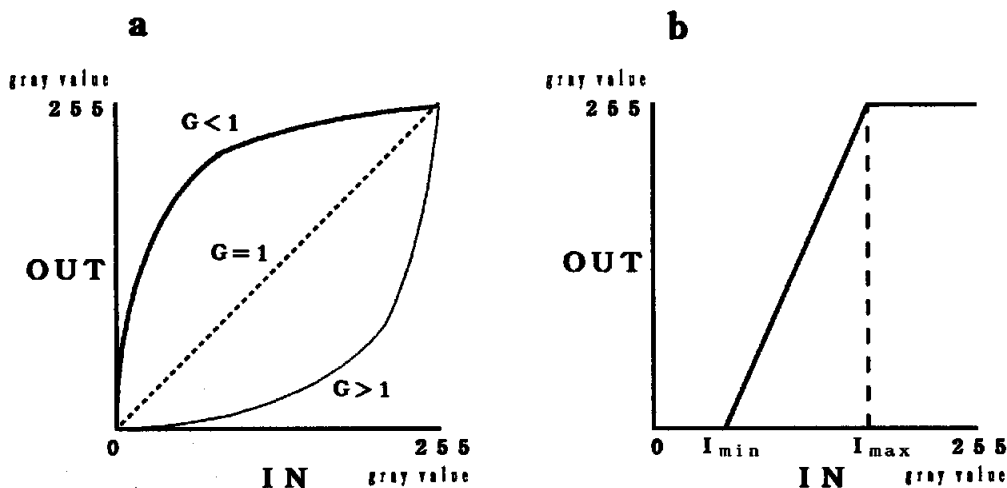


Fig. 2 Relationships of gray levels between before and after histogram transformation. Gray values of an input image (IN) were replaced by the operation for gamma correction (a) or for histogram stretch (b). In the gamma correction, when a parameter (G) is less than 1, contrast of a part of the low gray values in the input image is enhanced, whereas when G is more than 1, contrast of a part of the high gray values is enhanced. In the histogram stretch, contrast of the input image is enhanced by stretching gray values distributed between I_{min} and I_{max} from 0 (=black) to 255 (=white).

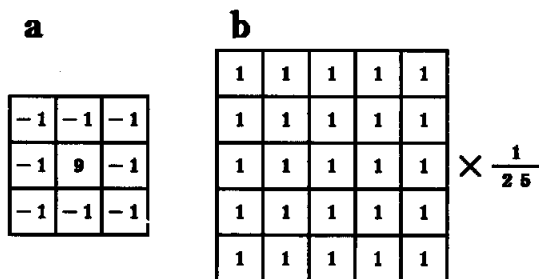


Fig. 3 Convolution masks for spatial filtering. The 3×3 convolution mask for sharpening filter (a) and the 5×5 convolution mask for smoothing filter (b). The operation of the sharpening filter has the effect of enhancing edges of specimens. The smoothing filter removes higher frequency components such as noises occurring in images by averaging gray values of neighboring 5×5 pixels.

To remove from the images the partition patterns of the optical fibers constituting the fiber-optic plate, spatial frequency components of the pattern were analyzed by a two-dimensional fast Fourier transform (FFT) technique. Then the two-dimensional inverse FFT was performed to obtain the processed image.⁵ The averaging filter was also tried for use in removing the patterns.

Results

The NG108-15 cells stained with Acridine Orange could be visualized easily with the fiber-optic plate

microscope system. A typical image is shown in Fig. 4a. Although the shape of a whole cell was recognizable, the image of one frame, that is, the raw image, appeared to be rough due to presence of random noise. In this image, it was difficult to observe the tips of the nerve fibers because of the poor contrast to the background. To improve the image, the sequence of image processing techniques shown in Fig. 1a was performed.

Integration of the 64 consecutive frames of this image considerably reduced the effect of random noise and the contours of the cell were detected clearly (Fig. 4b). Since the image was obtained by summing up the consecutive frames, it seemed that the distribution of the random noises was temporally averaged out.

Subsequently, the integrated image was processed by the histogram transformation techniques for improving the contrast. The gamma correction enhanced the contrast of parts of the low gray level, such as the peripheral areas of the cell. In this operation, the distribution of nerve fibers extending from the cell body became recognizable up to their tips (Fig. 4c). The histogram stretch further improved the contrast of the whole image by lowering the gray values of the background area to nearly a black level and by stretching the range of gray levels where gray values of the cell area were included (Fig. 4d). Compared with the raw image, this image was significantly improved, with higher contrast and a lower noise level.

The sharpening filter was also used on the processed image. This operation somewhat braced the image of the cell by enhancing its contour, but the noise edges were also enhanced. Components of high spatial frequency derived from the partitions of the optical fibers con-

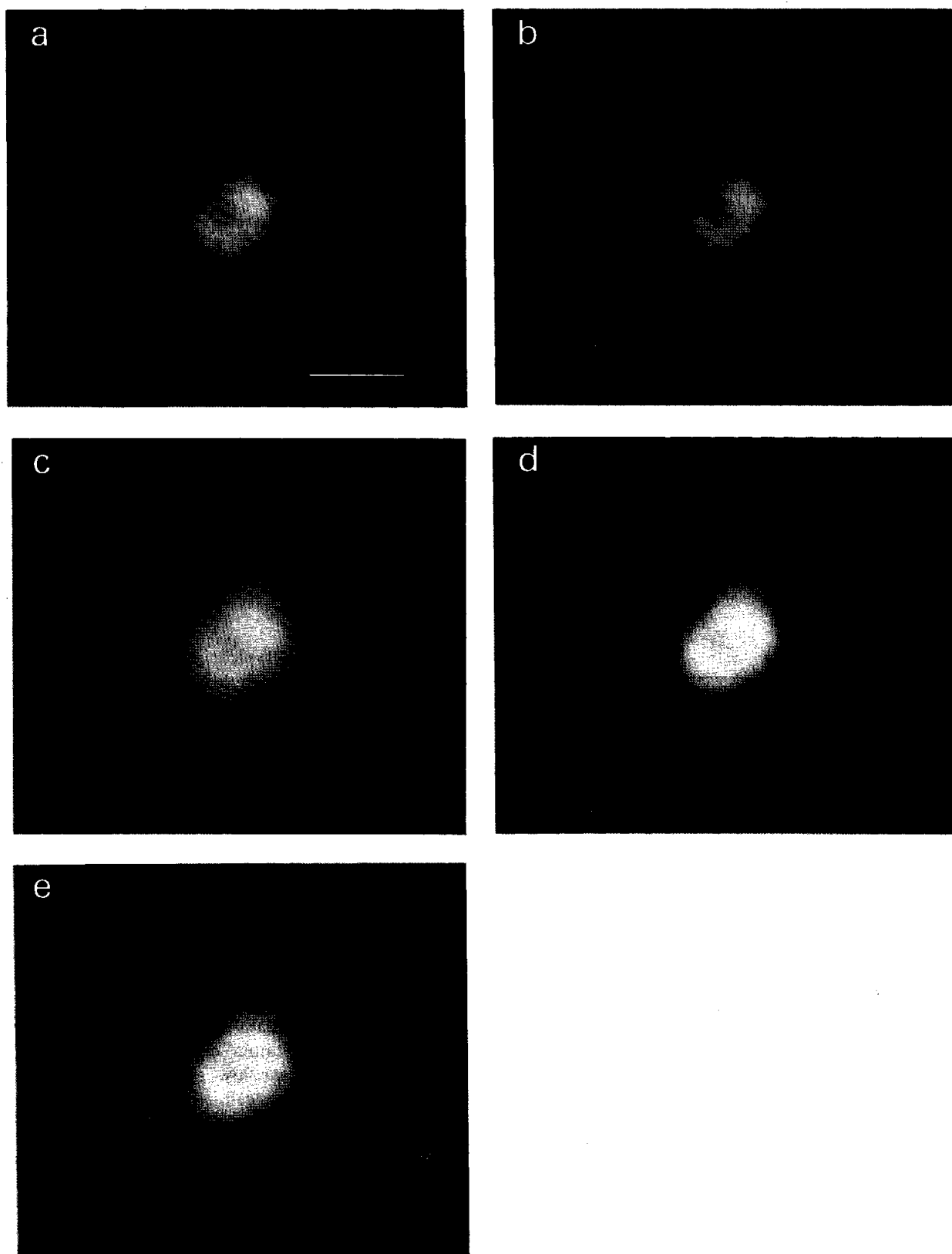


Fig. 4 Effects of digital image processing techniques on the fluorescence image of a static specimen. a. One frame of an image of the NG108-15 cell was acquired. The cell was stained with Acridine Orange. b. Sixty-four consecutive frames of the image were integrated. c. The integrated image (image b) was processed by gamma correction ($G=0.6$). d. Image c was processed by histogram stretch ($I_{\min}=20$, $I_{\max}=180$). e. Image d was further processed by the sharpening filter. Bar in a, 50 μm .

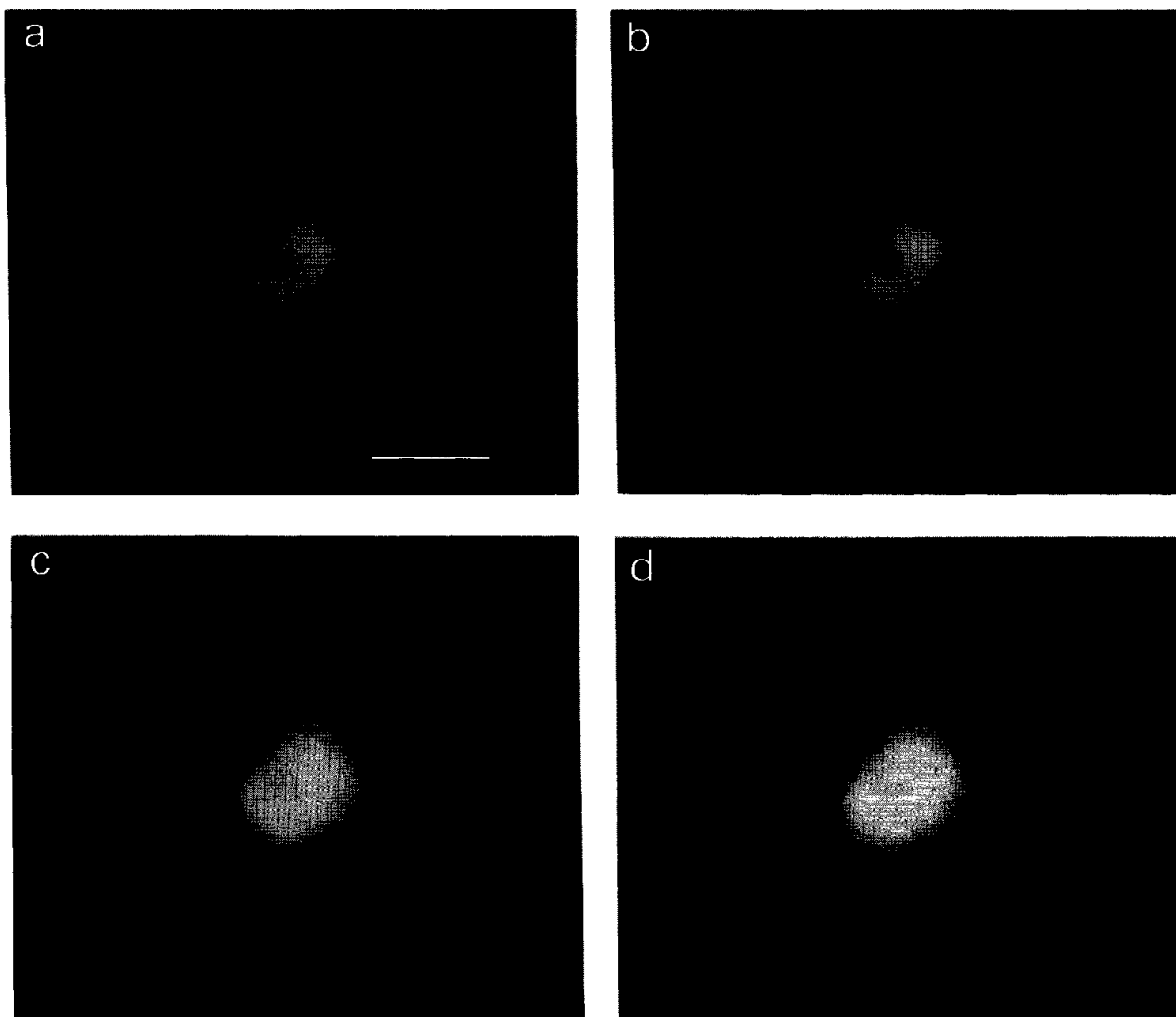


Fig. 5 Effects of digital image processing techniques on the fluorescence image of a moving specimen. a. One frame of an image of the NG108-15 cell was acquired. This is the same image as Fig. 4a. b. The image was processed by the averaging filter. c. Image b was processed by gamma correction ($G=0.6$) and then by histogram stretch ($I_{\min}=15$, $I_{\max}=210$). d. Image c was further processed by the sharpening filter. Bar in a, 50 μm .

stituting the fiber-optic plate appeared on the cell. As a result, the processed image became rather noisy (Fig. 4e).

The integration of the 64 consecutive frames required about 2 s for acquiring an image. It is ineffective in observations of moving specimens, since this method cancels out not only random noises but also any movements faster than the integration time. For those kinds of cases, the smoothing filters were used for reducing noise seen in the raw image (Fig. 1b). The averaging filter effectively reduced the random noise (Fig. 5b). In this manner, the distribution of the random noise would be spatially averaged out. A similar effect was obtained with the median filter (data not shown), but these operations resulted in a blurring of the original image. It took longer to complete processing of the median filter (approx. 20 min/image) than

to complete processing of the averaging filter (approx. 4 min/image). Because of the processing time delay, the median filter was thought less practical. After the filtering operation, the same techniques were available for the histogram transformation and for the sharpening filter as those used on the integrated image. By means of these techniques, similar effects on the contrast enhancement were obtained (Figs. 5c & d).

In the image processed by the sharpening filter, the partition patterns of optical fibers were enhanced (Fig. 4e). These partitions corresponded to the dead space of the fiber-optic plate. For a proper presentation of the image, two image processing techniques were tried in order to remove the patterns. To detect the pattern clearly, fluorescent beads were imaged. The fluorescence of the beads was more intense than that of the

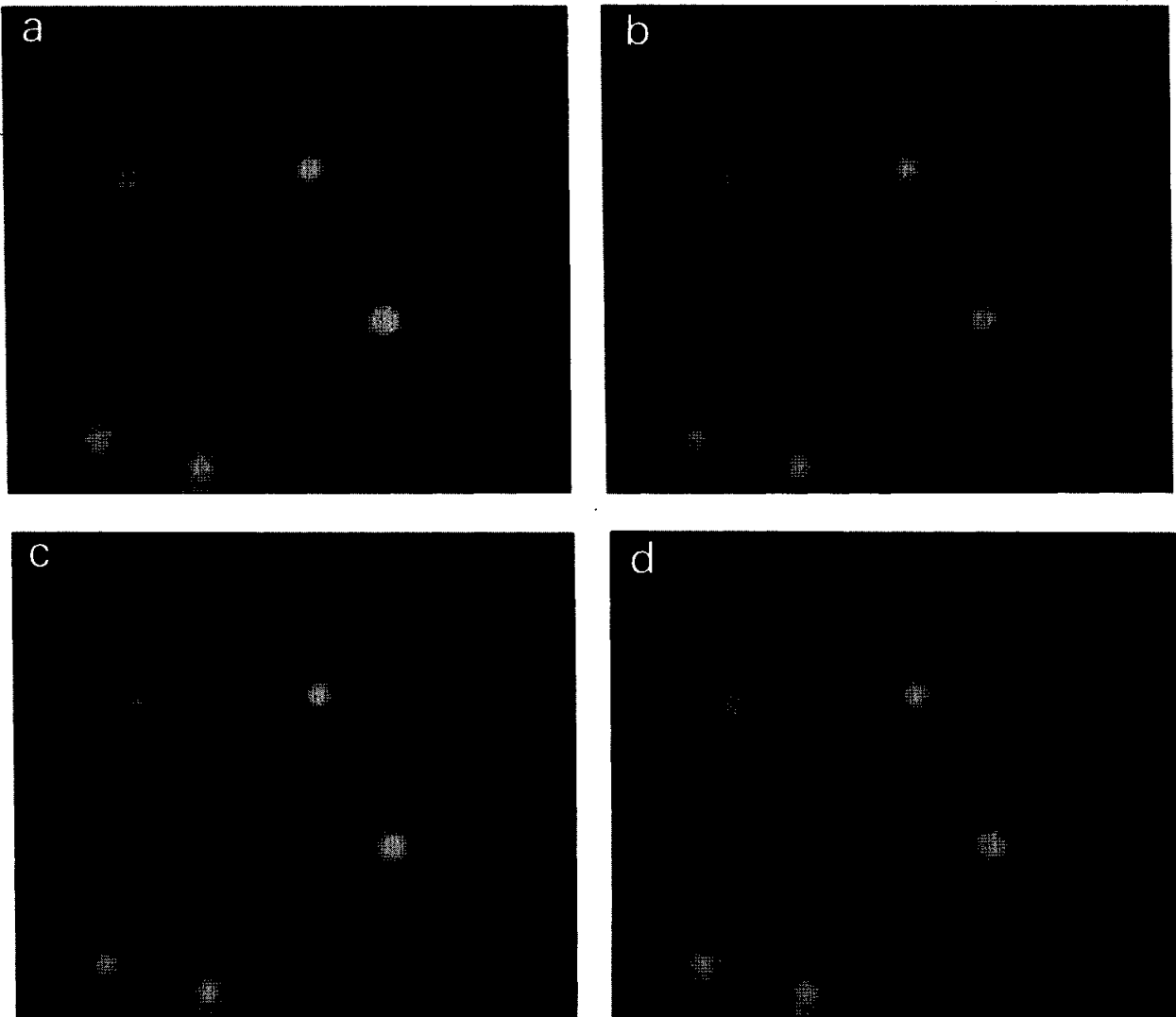


Fig. 6 Effects of image processing on removal of the partition patterns of optical fibers. a. Original image. Fluorescent beads were imaged by integration of 64 consecutive frames. The dark grid-like patterns overlapping the beads are partitions of optical fibers. b. The original image was processed by the 5×5 averaging filter. c. The original image was also processed by the two-dimensional FFT. d. The same fluorescent beads were imaged by slightly defocusing. All of the images are twice magnified by a function of the image processor.

cells and an image with higher contrast and a lower noise level was obtained. In the image, the grid-like partitions overlapping the beads were observed clearly (Fig. 6a). In this magnification, each partition was narrow enough to be removed with the smoothing filter of the 5×5 convolution mask without yielding marked blurring (Fig. 6b). With the two-dimensional FFT, the pattern was also removed quite well (Fig. 6c). As a time-saving method that required no image processing, the same fluorescent beads were imaged under the condition that the distance between the fiber-optic plate and the objective be approximately $10 \mu\text{m}$ further than what it was while in focus. Although this imaging never eliminated out-of-focus blurs in the image, the effect of the patterns was considerably reduced (Fig. 6d).

Discussion

It was found that the fiber-optic plate microscope system had sufficient sensitivity to detect cells stained with a fluorescent dye, but the raw image was noisy. The signal-to-noise ratio of an image depends on the brightness of the specimen, noise level of a video camera, time for integrating frames *etc.* In this system, narrowness of the diameter of the optical fibers contributes to the weakening of the specimen's fluorescence.

Most of the digital image processing techniques performed here were effective in improving the image. For imaging of static specimens such as the NG108-15 cells, integration of frames for a few seconds is an effective method for storing the image into a frame

memory while reducing the effect of random noise. Integration has the effect of increasing the signal-to-noise ratio of the image in proportion to the square root of the number of the integrated frames.^{6,7}

After image acquisition is completed, if the contrast between the specimen and background is not remarkable, digital contrast enhancement should be performed to make the image clear. Gamma correction could enhance the contrast of a specimen lost in a dark background. This operation seems to be effective for low light images, especially those acquired by the fiber-optic plate microscope. The histogram stretch also enhanced the contrast by making the best of the dynamic range of 8 bit gray levels.

When further sharpening of the images is required, spatial filtering can be used. The sharpening filter has been used for the purposes of removing blurred components from an image and for enhancement of edges of specimens. In this study, however, the sharpening filter also caused enhancement of noises or of the partition patterns of the optical fibers. The sharpening filter is probably more effective in enhancing edges of thinner or smaller structures such as cytoskeletons than for those that can be visualized with the resolution of this system.

When specimens of intense fluorescence such as fluorescent beads were observed, the dark patterns of the partitions also made the image unsightly. Such patterns were removed significantly in this study by use of the smoothing filter. Observation with a higher magnification however will cause enlargement of the dead space of the fiber-optic plate. In such cases, convolution masks of wider sizes should be used, but this results in prolix processing. It is also feared that this operation alters the original shape and light intensity of the specimen. Because the patterns are fixed and appear periodically, the two-dimensional FFT seems the most reasonable method for removing them without altering the original shape and light intensity of the specimen regardless of the magnification.

For observations of dynamic specimens, the image processing techniques described above should be performed in real time. For continuous observations, various temporal averaging functions which average successive frames have been used to reduce random noises.^{7,8} For example, a rolling average function outputs an image of a weighted average of the last input image and a previously stored image, whereby an effect similar to the image integration is obtained for the images of moving specimens.

But these methods result in lowering the temporal resolution, so that motions and changes in light intensity of a specimen occurring faster than the averaging period will not appear. When observations of fast changes with noise reduction is required, spatial noise filtering

after image acquisition done by freezing just one frame is an advisable method. This method methodologically sacrifices the spatial resolution of the image. But the spatial resolution of this system is in effect limited by the diameter of the optical fibers. In the magnification of the 40× objective, the resolution determined by the diameter of the optical fibers was inferior to that of the frame memory. It was therefore not thought that the actual resolution of the image processed by spatial filtering with a 5×5 convolution mask became significantly lower.

Until now, many types of elaborate image processing techniques have been developed for studies on cell biology. For example, removal of out-of-focus information from images for three-dimensional, optical sectioning microscopy⁹ and ratio imaging for measuring intracellular calcium ion concentration.¹⁰ It is evident that a considerable number of calculations have to be done for completing these operations. The time required by image processing makes it difficult to observe and analyze the dynamic processes in real time. In such cases, it is desirable that a image processor with higher performance be used to speed up these image processing techniques.

We thank Mr. H. Tsuchiya (Hamamatsu Photonics, K. K.) for his valuable support and comments on implementation of the two-dimensional FFT.

References

1. M. Hirano, Y. Yamashita and A. Miyakawa, *Anal. Sci.*, **9**, 375 (1993).
2. T. M. Cannon and B. R. Hunt, *Scientific American*, **245**, 4, 136 (1981).
3. S. Inoué, "Video Microscopy", p. 327, Plenum Press, New York, 1986.
4. M. Nirenberg, S. Wilson, H. Higashida, A. Rotter, K. Krueger, N. Busis, R. Ray, J. G. Kenimer and M. Adler, *Science* [Washington, D.C.], **222**, 794 (1983).
5. B. Jähne, "Digital Image Processing", p. 53, Springer-Verlag, Berlin, 1991.
6. R. D. Allen and N. S. Allen, *J. Microsc.*, **129**, 3 (1983).
7. D. G. Weiss, W. Maile and R. A. Wick, "Light Microscopy in Biology", ed. A. J. Lacey, p. 221, IRL Press, Oxford, 1989.
8. T. Salmon, R. A. Walker and N. K. Pryer, *BioTechniques*, **7**, 624 (1989).
9. D. A. Agard, Y. Hiraoka, P. Shaw and J. W. Sedat, *Meth. Cell Biol.*, **30**, 353 (1989).
10. R. Y. Tsien and A. T. Harootunian, *Cell Calcium*, **11**, 93 (1990).

(Received March 9, 1993)

(Accepted May 10, 1993)